Synthesis, Magnetic Properties, and Catalytic Properties of a Nickel(II)-Dependent Biomimetic of Metallohydrolases

Adolfo Horn Jr.[1]*, Daniel Englert[2,3], Asha E. Roberts[2], Peter Comba[2], Gerhard Schenk[3†], Elizabeth H. Krenske[3] and Lawrence R. Gahan[3]*

[1] Laboratório de Ciências Químicas, Universidade Estadual do Norte Fluminense Darcy Ribeiro, Campos dos Goytacazes, Brazil, [2] Anorganisch-Chemisches Institut and Interdisciplinary Center of Scientific Computing, Universität Heidelberg, Heidelberg, Germany, [3] School of Chemistry and Molecular Biosciences, The University of Queensland, Brisbane, QLD, Australia

A dinickel(II) complex of the ligand 1,3-bis(bis(pyridin-2-ylmethyl)amino)propan-2-ol (HL1) has been prepared and characterized to generate a functional model for nickel(II) phosphoesterase enzymes. The complex, $[Ni_2(L1)(\mu\text{-OAc})(H_2O)_2](ClO_4)_2 \cdot H_2O$, was characterized by microanalysis, X-ray crystallography, UV-visible, and IR absorption spectroscopy and solid state magnetic susceptibility measurements. Susceptibility studies show that the complex is antiferromagnetically coupled with the best fit parameters $J = -27.4$ cm^{-1}, $g = 2.29$, $D = 28.4$ cm^{-1}, comparable to corresponding values measured for the analogous dicobalt(II) complex $[Co_2(L1)(\mu\text{-OAc})](ClO_4)_2 \cdot 0.5\,H_2O$ ($J = -14.9$ cm^{-1} and $g = 2.16$). Catalytic measurements with the diNi(II) complex using the substrate bis(2,4-dinitrophenyl)phosphate (BDNPP) demonstrated activity toward hydrolysis of the phosphoester substrate with $K_m \sim 10$ mM, and $k_{cat} \sim 0.025$ s^{-1}. The combination of structural and catalytic studies suggests that the likely mechanism involves a nucleophilic attack on the substrate by a terminal nucleophilic hydroxido moiety.

Keywords: nickel, phosphoesterase, magnetism, DFT, kinetics, mechanism

INTRODUCTION

Our understanding of the bioinorganic significance of nickel can be traced to the discovery that the specific activity of the soluble jack bean urease, after partial EDTA-promoted inactivation, was a linear function of the nickel content, consistent with the presence of two nickel(II) ions per subunit of the pure enzyme (Dixon et al., 1980; Blakeley et al., 1982; Blakeley and Zerner, 1984). Previous to this discovery the importance of metal ions in general for the activity of urease was known, although the specific requirement for Ni(II) ions was not (Jacoby, 1933; Shaw, 1954; Shaw and Raval, 1961; Spears et al., 1977). Subsequently it was recognized that nickel is also required for the enzymatic activity of carbon monoxide dehydrogenase, (Ensign et al., 1989, 1990; Shin and Lindahl, 1992; Gencic and Grahame, 2003) and plays an important role in other bioinorganic systems, (Ashwini, 2006) including [NiFe]-hydrogenase (Przybyla et al., 1992; Sargent, 2016; Vaissier and Van, 2017) and a nickel dependent superoxide dismutase (Barondeau et al., 2004). In contrast to other bioinorganic systems Ni(II) complexes have received less attention. A limited number of studies have focussed on di-Ni(II) model complexes for urease (Meyer, 2009) and FeNi complexes
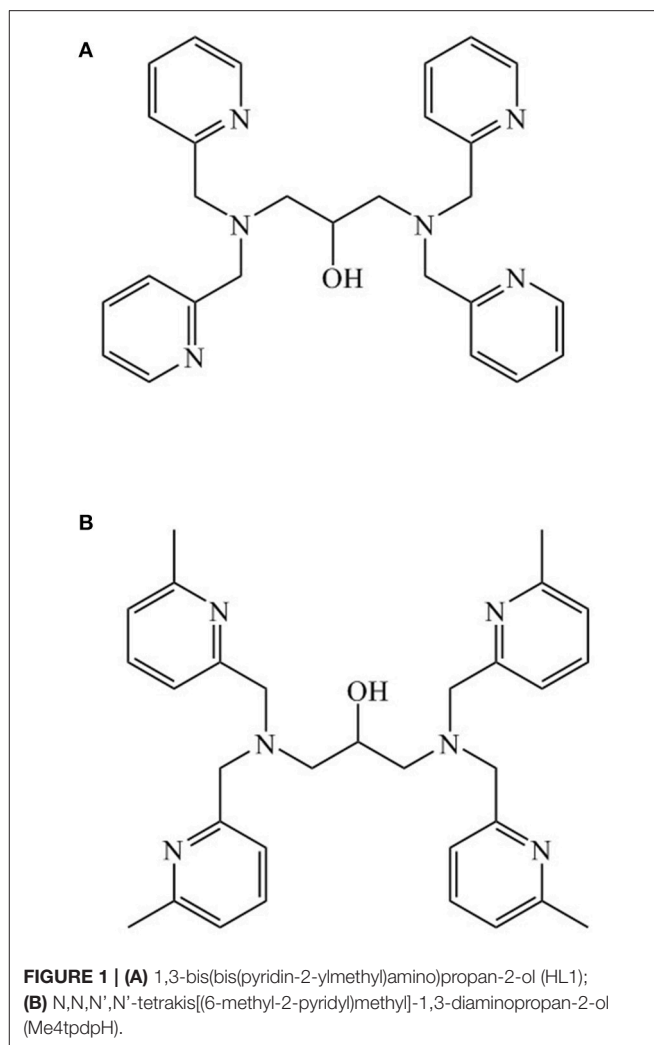
for hydrogenases (Vaissier and Van, 2017), and Neves and colleagues have developed several Ni(II) models for phosphatases, in particular purple acid phosphatases (PAPs) (Greatti et al., 2008; Piovezan et al., 2012; Xavier and Neves, 2016). PAPs present an ideal system to study biomimetics, in parts because of the wealth of sequence (Flanagan et al., 2006), structural and functional data available (Schenk et al., 2013), but also because these enzymes occur in homo- and hetero-bimetallic form in nature, using a range of metal ions (Fe, Zn, Mn; Mitić et al., 2009, 2010). Furthermore, the Fe(III)Ni(II) form of PAP is catalytically active, one of the few known metallohydrolases that can accommodate Ni(II) and maintain functionality (Schenk et al., 2008). This flexibility of PAPs with respect to their use of metal ions may be a reflection of their dual function as a phosphatase and peroxidase; indeed, in its di-Fe(III) form PAP is easily and reversibly reduced to the heterovalent Fe(III)Fe(II) form (redox potential ~340 mV), a process that allows the enzyme to act as a Fenton catalyst (Sibille et al., 1987; Bernhardt et al., 2004).

The metal ion composition of PAP may also influence its reaction mechanism; in particular, the identity of the hydrolysis-initiating nucleophile may be affected by the identity of the metal ions (Mitić et al., 2010; Selleck et al., 2017). Here, we selected ligand 1,3-bis(bis(pyridin-2-ylmethyl)amino)propan-2-ol (**Figure 1**) to probe the possibility that a di-Ni(II) biomimetic may promote phosphatase activity. This ligand, previously used to generate a di-Mn(II) system (Suzuki et al., 1989; Sato et al., 1992), offers an opportunity to investigate the hydrolytic mechanism as it offers a limited number of possible pathways for the nucleophile.

EXPERIMENTAL SECTION

General Methods

Chemicals were purchased from Sigma-Aldrich, Merck, ABCR, Acros or Alfa Aeser and used without further purification. Reactions requiring the exclusion of moisture and/or oxygen were carried out under nitrogen atmosphere using standard Schlenk techniques. TLC was performed on TLC Silica gel 60 F_{254} TLC plates purchased from Merck and visualization of the spots was carried out by fluorescence quenching with 254 nm UV light. Purification of raw products by column chromatography were performed using silica gel (grade 9385, 60 Å, 230–400 mesh size) purchased from Sigma-Aldrich. NMR spectra were recorded with a Bruker Avance III 300 system at 300 K. Chemical shifts (δ) are given in ppm and coupling constants (J) in Hz. ^{1}H and ^{13}C spectra were referenced to the protio impurity or the ^{13}C signal of the deuterated solvent. Abbreviations used for observed multiplicities are d for doublet, dd for doublet of doublets, td for triplet of doublets and m for multiplet. IR spectra were measured with a Perkin Elmer Frontier FT-IR spectrometer, transmittance data are given in wave number $\tilde{\nu}$ (cm^{-1}). Abbreviations used for observed intensities are w for weak, m for medium and s for strong. UV-Vis absorption spectra were recorded with an Agilent Technologies Cary 60 UV-Vis spectrophotometer. Elemental analyses were performed by the elemental microanalysis service at the School of Chemistry & Molecular Biosciences of the

FIGURE 1 | (A) 1,3-bis(bis(pyridin-2-ylmethyl)amino)propan-2-ol (HL1); **(B)** N,N,N',N'-tetrakis[(6-methyl-2-pyridyl)methyl]-1,3-diaminopropan-2-ol (Me4tpdpH).

University of Queensland. The synthesis of the cobalt(II) complex, $[Co_2(L1)(\mu\text{-}OAc)](ClO_4)_2 \cdot 0.5\, H_2O$, is described in the **Supplementary Material**.

Hydrolysis Studies

Kinetic studies were conducted using a Varian Cary50 Bio UV/Visible spectrophotometer with a Peltier temperature controller (25°C) and 10-mm quartz cuvettes, and employing bis-(2,4-dinitrophenol)phosphate (BDNPP) as substrate. Assays were measured in a solvent system composed of 50:50 acetonitrile:buffer. An aqueous multicomponent buffer was employed made up of 50 mM 2-(N-morpholino)ethanesulfonic acid (MES), 4-(2-hydroxyethyl)-1-piperazineethanesulfonic acid (HEPES), 2-(N-cyclohexylamino)ethane sulfonic acid (CHES) and N-cyclohexyl-3-aminopropanesulfonic acid (CAPS), with ionic strength controlled with LiClO$_4$ (250 mM). The pH values reported for the buffers are those of the aqueous component (Kaminskaia et al., 2000). The initial-rate method was employed and assays were measured such that the initial linear portion of the data was used for analysis. Product formation was determined by monitoring the formation of 2,4-dinitrophenolate; the

extinction coefficient of this product at 400 nm varies from 7,180 at pH 4.5, 10,080 at pH 5.0; 11,400 at pH 5.5 to 12,000 at 6.0 and 12,100 at pH 6.5–11 (Smith et al., 2007). Assays to evaluate the pH dependence of the reaction contained 40 μM complex and 5 mM BDNPP; to evaluate the effect of [substrate], 0.5 mM complex was mixed with 1–11.5 mM BDNPP. Catalytic rates could be measured reliably up to pH 11.0 and were fit to the simplest possible model to describe the pH dependence of the observed catalytic rates (Kantacha et al., 2011). The model invokes one relevant protonation equilibrium and is described by an equation of the form

$$y(x) = \frac{a}{1 + \frac{x}{b}}$$

Here, a and b represent fitting parameters (i.e., $V_{\max}$ and K_a, respectively), while x is the variable ([H^+] in this case) for a function of y (representing the measurable catalytic rate v). At very high [H^+] (low pH; x/b>>0) the denominator is >>$V_{\max}$ and hence the rate is approximating 0. At very low [H^+] (high pH; x/b~0) the denominator approximates 1 and hence the rate approaches $V_{\max}$. The fitting parameter b, representing the relevant acid dissociation constant K_a, is thus the [H^+] where the rate v reaches half of its maximum value $V_{\max}$.

The catalytic rates were measured as a function of substrate concentration. Experimental limitations (imposed by the solubility of the substrate) prevented accurate measurements above 6 mM. The data displayed hyperbolic behavior but saturation was not achieved. Consequently, the data were analyzed with a combination of non-linear regression and double-reciprocal linear fits, using the Michaelis-Menten equation

$$v_0 = \frac{V_{max}[S]}{K_m + [S]},$$

where V_0 is the initial rate, V_{max} is the maximum rate, K_M is the Michaelis constant, and [S] is the substrate concentration.

Susceptibility Measurements

The magnetic data were collected using an MPMS-XL 5T (Quantum Design) SQUID magnetometer. Fixed powder samples were prepared by pressing the powder into PTFE tape to prevent field-induced reorientation. Data were corrected for contributions of the sample holders and, using Pascal's constants (Bain and Berry, 2008), for the diamagnetic contributions of the samples. Effective magnetic moments were calculated using the relationship $\mu_{\text{eff}} = 2.828(\chi_M T)^{1/2}$.

Crystallographic Measurements

Crystallographic data for the complex were collected at 190(2) K using an Oxford Diffraction Gemini Ultra dual source (Mo and Cu) CCD diffractometer with Mo ($\lambda_{K\alpha} = 0.71073$ Å) radiation. The structure was solved by direct methods (SIR-92) and refined by full matrix least squares methods (SHELXL 97) based on F^2 (Sheldrick, 1997), accessed through the WINGX 1.70.01 crystallographic collective package (Farrugia, 1999). Hydrogen atoms were fixed geometrically and not refined. X-ray data

of the published structure was deposited with the Cambridge Crystallographic Data Centre, CCDC 1844565.

Computational Details

Geometry optimizations of the cations of [Ni$_2$(L1)(μ-OAc)(H$_2$O)$_2$](ClO$_4$)$_2$·H$_2$O and [Co$_2$(L1)(μ-OAc)](ClO$_4$)$_2$·0.5H$_2$O were undertaken with the Gaussian 09 set of programs (Frisch et al., 2013) starting from the X-ray structural data. The B3LYP functional (Becke, 1993), Noodleman's broken symmetry, (Noodleman et al., 1988) the TZV basis set (Schaefer et al., 1992). Orca 2.6.04 (Neese, 2012) was used for the magnetic coupling constant calculation essentially as described previously (Comba et al., 2009).

Synthesis

1,3-Bis(Bis(Pyridin-2-ylmethyl)Amino)Propan-2-ol (HL1)

2-(Chloromethyl)pyridine hydrochloride (4.00 eq, 6.01 g, 36.62 mmol) was dissolved in 3 mL distilled water and 15 mL of an aqueous 5 M NaOH solution was added while stirring. 1,3-diaminopropan-2-ol (1.00 eq, 825 mg, 9.15 mmol), 15 mL of 5 M NaOH solution and tetraoctylammonium bromide (0.02 eq, 100 mg, 183 μmol) were then added. The resulting red mixture was stirred at room temperature overnight. The reaction mixture was transferred into a separatory funnel with 40 mL chloroform, 40 mL of brine, the aqueous phase was extracted twice with 10 mL chloroform, and the combined organic layers washed with 50 mL water. The separated organic layer was dried over magnesium sulfate, filtered and concentrated under reduced pressure. The crude product was purified using a MeOH-equilibrated silica column (Merck) according to the manufacturer's instructions. After removal of the solvent under reduced pressure the product was obtained as orange oil (88%, 3.66 g, 8.05 mmol). ^{1}H NMR (300 MHz, CDCl$_3$): δ 8.49–8.45 (4H, m), 7.54 (4H, td, $J = 11.5$ Hz, $J = 1.8$ Hz), 7.37–7.31 (4H, m), 7.12–7.05 (4H, m), 4.03–3.92 (1H, m), 3.89 (4H, d, $^2J = 14.7$ Hz), 3.84 (4H, d, $^2J = 14.7$ Hz), 2.69 (2H, dd, $^2J = 13.3$ Hz, $^3J = 4.1$ Hz), 2.59 (2H, dd, $^2J = 13.3$ Hz, $^3J = 7.8$ Hz) ppm. ^{13}C NMR (75 MHz, CDCl$_3$): δ 159.3, 149.0, 136.5, 123.2, 122.1, 67.2, 60.8, 59.1 ppm.

[Ni$_2$(L1)(μ-OAc)(H$_2$O)$_2$](ClO$_4$)$_2$·H$_2$O

Nickel(II) acetate tetrahydrate (2.00 eq, 109.5 mg, 440 μmol) was dissolved in 6 mL MeOH. Lithium perchlorate trihydrate (4.00 eq, 153.4 mg, 880 μmol) and 4 mL of a methanol solution of 1,3-bis(bis(pyridin-2-ylmethyl)amino)propan-2-ol (HL1) (1.00 eq, 100.0 mg, 220 mmol) were added and the reaction mixture stirred under reflux for 1 h. Upon cooling to room temperature, the solvent was removed under reduced pressure and the resulting product was recrystallized in a water/acetone mixture resulting in blue crystals (46%, 89.6 mg). IR: $\tilde{\nu} = 3489$ (w), 3221 (w), 2801 (w), 1651 (m), 1606 (s), 1548 (s), 1482 (m), 1445 (s), 1427 (s), 1287 (m), 1161 (m), 1070 (s), 1056 (s), 1037 (s), 1023 (s), 990 (m), 928 (m), 886 (m), 760 (s), 620 (s) cm^{-1}. UV/vis $\lambda_{\max}$ (ε), 950 nm (57 M^{-1}cm^{-1}), 590 nm (43 M^{-1}cm^{-1}). Calc. for C$_{29}$H$_{38}$Cl$_2$N$_6$Ni$_2$O$_{14}$: C, 39.45; H, 4.34; N, 9.52 %. Found: C, 39.49; H, 4.13; N, 9.37%.

RESULTS AND DISCUSSION

Syntheses

The ligand 1,3-bis(bis(pyridin-2-ylmethyl)amino)propan-2-ol (HL1) was prepared by a modification of previously described procedures (Suzuki et al., 1989; Sato et al., 1992). The nomenclature HL1 indicates that the ligand is protonated at the hydroxido moiety and on formation of the complex the ligand is deprotonated and coordinates as the monoanion $L1^-$. We have reported previously a diZn(II) complex with $L1^-$ as a functional model for zinc(II) phosphoesterase enzymes (Mendes et al., 2016).

In this work the dinuclear nickel complex $[Ni_2(L1)(\mu\text{-}OAc)(H_2O)_2](ClO_4)_2 \cdot H_2O$ was synthesized from a reaction of HL1 with two equivalents of nickel(II) acetate in methanol

TABLE 1 | Crystallographic data for $[Ni_2(L1)(\mu\text{-}OAc)(H_2O)_2](ClO_4)_2 \cdot H_2O$.

Complex	$[Ni_2(L1)(\mu\text{-}OAc)(H_2O)_2](ClO_4)_2 \cdot H_2O$
Empirical formula	$C_{29}H_{36}Cl_2N_6Ni_2O_{13}$
Formula weight	864.96
Wavelength (Å)	0.71073 (Mo K_α)
Crystal system	Monoclinic
Space group	C 2/c
a (Å)	12.7975(10)
b (Å)	21.0734(13)
c (Å)	13.8612(8)
α (°)	90
β (°)	105.169(7)
γ (°)	90
Vol (Å^3)	3,607.9(4)
Z	4
μ (mm^{-1})	1.263
F(000)	1,784
ρ (Mg/m^3)	1.592
Reflns col.	8510
Ind. Reflns (R_{int})	3,178(0.0533)
θ range (°)	3.48 to 25.00
GOOF on F^2	1.042
final R indices [I>2σ(I)]	R1 = 0.0523, wR2 = 0.1171
R indices (all data)	R1 = 0.0733, wR2 = 0.1312

TABLE 2 | Selected bond lengths (Å) and angles (°) for $[Ni_2(L1)(\mu\text{-}OAc)(H_2O)_2](ClO_4)_2 \cdot H_2O$.

N(1)-Ni(1) 2.078(3)	N(2)-Ni(1) 2.110(4)	N(3)-Ni(1) 2.080(4)
O(1)-Ni(1) 1.990(2)	O(2)-Ni(1) 2.058(3)	O(3)-Ni(1) 2.132(3)
Ni(1)-O(1)-Ni(1) 131.6(2)	O(1)-Ni(1)-O2 93.57(13)	O(1)-Ni(1)-N(1) 96.25(10)
O(2)-Ni(1)-N(1) 97.99(13)	O(1)-Ni(1)-N(3) 92.40(10)	O(2)-Ni(1)-N(3) 99.49(13)
N(1)-Ni(1)-N(3) 159.95(14)	O(1)-Ni(1)-N(2) 83.55(14)	O(2)-Ni(1)-N(2) 176.71(13)
N(1)-Ni(1)-N(2) 80.79(14)	N(3)-Ni(1)-N(2) 82.26(14)	O(1)-Ni(1)-O(3) 176.18(12)
O(2)-Ni(1)-O(3) 89.54(12)	N(1)-Ni(1)-O(3) 85.50(13)	N(3)-Ni(1)-O(3) 84.89(12)
N(2)-Ni(1)-O(3) 93.40(13)		

solution in the presence of $LiClO_4$. The nickel complex was obtained as bright blue crystals after recrystallization in a water/acetone mixture.

A complex with the same ligand and formulated as $[Ni_2(L1)(\mu\text{-}OAc)_2](PF_6) \cdot MeOH$ has been reported previously (Moffat et al., 2014). In that case the synthesis involved the reaction of the ligand HL1, nickel(II) acetate in methanol, in the presence of triethylamine and $NaPF_6$ under reflux. On standing at $-18°C$ the pink crystals which initially formed were removed, the mother liquor collected and concentrated under vacuum and upon slow diffusion of diethylether on standing the deep blue crystals of $[Ni_2(L1)(\mu\text{-}OAc)_2](PF_6) \cdot MeOH$ were collected and structurally characterized (Moffat et al., 2014). In addition, the Ni(II) complex of a similar ligand N,N,N',N'-tetrakis((6-methyl-2-pyridyl)methyl)-1,3-diaminopropan-2-ol (Me$_4$tpdpH), prepared by reaction of nickel(II) acetate, $NaClO_4$ with Me$_4$tpdpH in methanol at room temperature, and crystallized from a methanol/diethyl ether solution as light green crystals, has also been reported. The complex was formulated as $[Ni_2(Me_4tpdp)(\mu\text{-}OAc)(ClO_4)(CH_3OH)](ClO_4)$ (Yamaguchi et al., 1997, 2001). The synthesis and characterization of the cobalt complex $[Co_2(L1)(\mu\text{-}OAc)](ClO_4)_2$ has been reported previously (Siluvai and Murthy, 2009).

Spectroscopy

The infrared spectrum of $[Ni_2(L1)(\mu\text{-}OAc)(H_2O)_2](ClO_4)_2$ displayed bands attributed to the asymmetric and the symmetric acetate stretch ($\nu_{as} = 1,548$ cm^{-1}, $\nu_s = 1,445$ cm^{-1}), indicating the presence of a bridging acetate anion (Deacon and Phillips, 1980). Furthermore, characteristic bands at 1,606 cm^{-1} and 1,576 cm^{-1} were assigned to $\nu_{C=N}$ and $\nu_{C=C}$ of the pyridyl groups of the ligand, and those 1,070 cm^{-1} to the perchlorate counter ion.
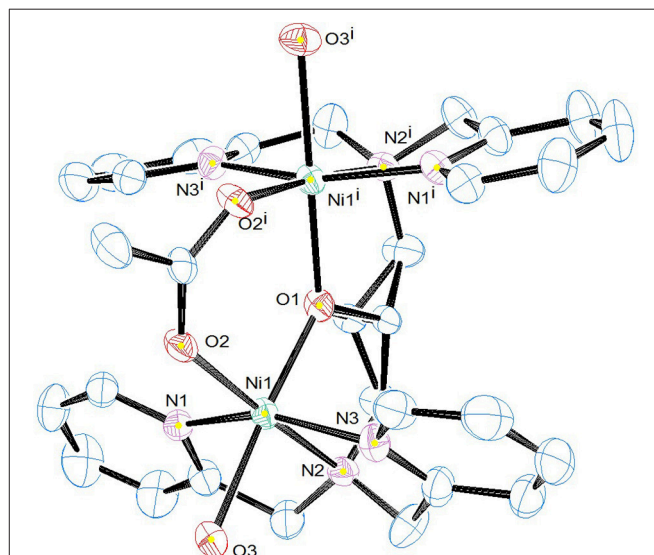

FIGURE 2 | ORTEP plot of the cation $[Ni_2(L1)(\mu\text{-}OAc)(H_2O)_2]^{2+}$. Counter ions and hydrogen atoms have been omitted for clarity (25% ellipsoid probability in ORTEP plot).

The electronic spectrum of $[Ni_2(L1)(\mu\text{-}OAc)(H_2O)_2](ClO_4)_2$ was measured in acetonitrile. For octahedrally coordinated Ni(II) ions there are three spin allowed d-d transitions from the $^3A_{2g}$ ground state to the higher excited triplet states $^3T_{2g}$, $^3T_{1g}$, and $^3T_{1g}$ (P). Spectral bands with maxima at 950 and 590 nm were assigned to the $^3A_{2g} \rightarrow \ ^3T_{2g}$ and $^3A_{2g} \rightarrow \ ^3T_{1g}$ transitions, respectively. The $^3A_{2g} \rightarrow \ ^3T_{1g}$ (P) transition is probably hidden under the intense band of the pyridyl groups with a maximum at 255 nm; a small shoulder around 400 nm could arise from this spin-allowed transition. A shoulder around 800 nm is assigned to the spin-forbidden d-d $^3A_{2g} \rightarrow \ ^1E_{1g}$ transition. The Racah parameter B and the ligand field splitting energy Dq of the d^8 Ni(II) system were determined using the bands of the $^3A_{2g} \rightarrow \ ^3T_{2g}$ and $^3A_{2g} \rightarrow \ ^3T_{1g}$ transitions and determined to be 877 and 1,053 cm^{-1}, respectively.

X-Ray Crystal Structure

Selected crystallographic data for $[Ni_2(L1)(\mu\text{-}OAc)(H_2O)_2](ClO_4)_2 \cdot H_2O$ are shown in **Table 1** and selected bond lengths and angles are displayed in **Table 2**. An ORTEP plot is shown in **Figure 2**. The structure is composed of the ligand mono-anion, two metal(II) ions and a bridging acetate with the Ni(II) structure containing two coordinated aqua ligands completing the hexacoordinate coordination sphere. The charge is balanced by perchlorate ions. In the diNi(II) complex there is disorder around the carbon atom of the bridging hydroxide. The coordination symmetry around each Ni(II) site for $[Ni_2(L1)(\mu\text{-}OAc)(H_2O)_2](ClO_4)_2 \cdot H_2O$ is octahedral and the donor set of both nickel atoms is N_3O_3, which is composed of a tertiary amino-N atom (Ni(1)-N(2): 2.110(4) Å), two pyridyl-N atoms (Ni(1)-N(1): 2.078(3) Å; Ni(1)-N(3): 2.080(4) Å), a bridging alkoxo-O atom (Ni(1)-O(1): 1.990(2) Å), an μ-acetato O atom (Ni(1)-O(2): 2.058(3) Å) and an O atom of a coordinating water molecule (Ni(1)-O(3): 2.132(3) Å). The bridging angle Ni-O(1)-Ni is 131.6° and the two nickel atoms are separated by a distance of 3.63 Å. The C(8) atom is disordered between two different positions.

For the previously reported complex $[Ni_2(L1)(\mu\text{-}OAc)_2](PF_6) \cdot MeOH$, the two Ni(II) octahedral sites are composed of two μ-acetate ligands, the three N donors of the L1 ligand, and the μ-O of the ligand (**Figure 3**, top; Moffat et al., 2014). The differences in the two diNi(II) structures of L1$^-$ involve the absence of the second bridging acetate ligand and the presence of the two terminal water molecules in $[Ni_2(L1)(\mu\text{-}OAc)(H_2O)_2](ClO_4)_2 \cdot H_2O$, as well as the presence of the ClO$_4^-$ anions. Furthermore, the coordinating groups present in the ligand arms show a meridional coordination mode, which induces the coordination of the water molecules in positions *anti* to each other.

The X-ray crystal structure of $[Ni_2(Me_4tpdp)(\mu\text{-}OAc)(ClO_4)(CH_3OH)](ClO_4)$ has been reported (**Figure 3**, bottom; Yamaguchi et al., 1997, 2001). The structure shows that both Ni(II) sites are six coordinate, the two metal ions separated by 3.62 Å and bridged by the ligand μ-O alkoxide and μ-acetato ligands. The sixth coordination site of one Ni(II) is made up of the O from a perchlorato ligand, whilst for the other metal ion a CH$_3$OH ligand completes the sixth coordination
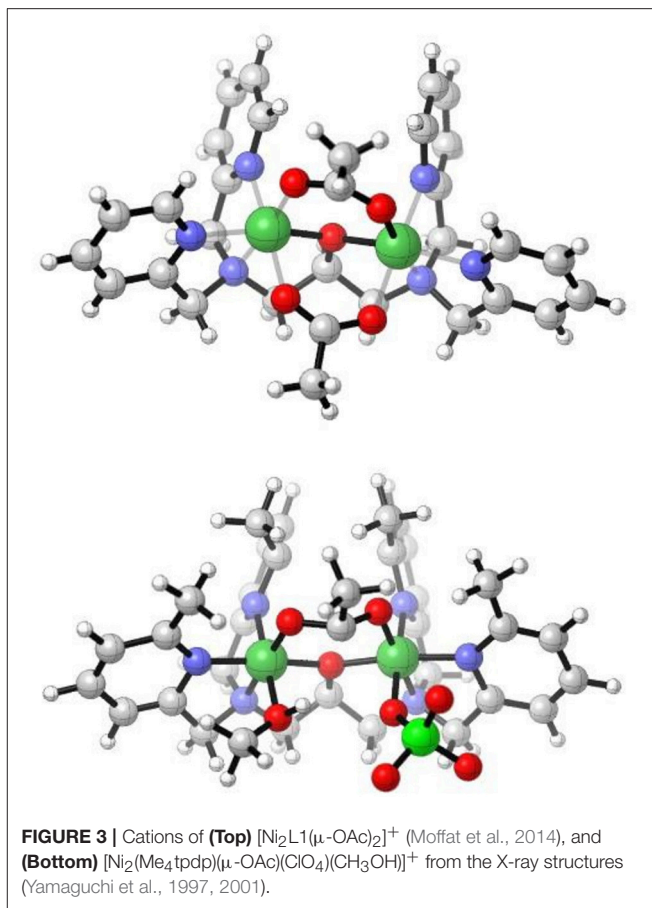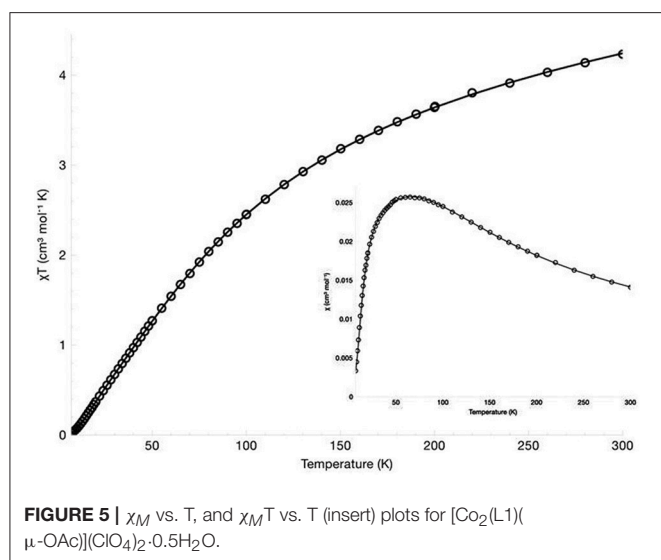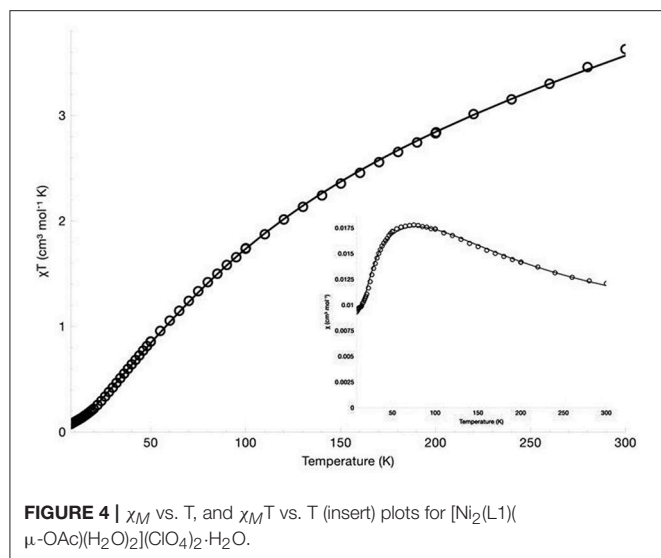

FIGURE 3 | Cations of **(Top)** $[Ni_2L1(\mu\text{-}OAc)_2]^+$ (Moffat et al., 2014), and **(Bottom)** $[Ni_2(Me_4tpdp)(\mu\text{-}OAc)(ClO_4)(CH_3OH)]^+$ from the X-ray structures (Yamaguchi et al., 1997, 2001).

(Yamaguchi et al., 1997, 2001). Whereas for the complex $[Ni_2(L1)(\mu\text{-}OAc)(H_2O)_2](ClO_4)_2 \cdot H_2O$ the coordinated aqua ligands are *trans* to the μ-alkoxo-O atom, effectively bisecting the two pyridyl rings of the ligand, this arrangement is not observed in the structure of the analogous $[Ni_2(Me_4tpdp)(\mu\text{-}OAc)(ClO_4)(CH_3OH)](ClO_4)$ complex. Here, the methanol and perchlorato ligands are located *cis* to the μ-alkoxo-O atom (Yamaguchi et al., 1997), and presumably replaced by aqua ligands in solution, an important consideration in subsequent hydrolytic studies (Yamaguchi et al., 2001).

The X-ray crystal structure of $[Co_2(L1)(\mu\text{-}OAc)](ClO_4)_2$ has been reported (Siluvai and Murthy, 2009). The structure shows a pseudo C_2-axis of symmetry with the μ-acetate ligand bridging the two Co(II) ions in a symmetric μ-1,3 mode. The two Co(II) sites display slightly distorted trigonal bipyramidal geometry with τ_{av}, the index of trigonality, equal to 0.93; a τ value of unity would perfect trigonal bipyramidal geometry (Addison et al., 1984; Siluvai and Murthy, 2009).

Magnetic Susceptibility

The magnetic susceptibility of the diNi(II) and diCo(II) complexes was measured over the temperature range 300 to 7 K in an applied field of 500 G. The χ_M vs. T, and $\chi_M T$ vs. T plots are presented in **Figure 4** for $[Ni_2(L1)(\mu\text{-}OAc)(H_2O)_2](ClO_4)_2 \cdot H_2O$

FIGURE 4 | χ_M vs. T, and χ_MT vs. T (insert) plots for [Ni$_2$(L1)(μ-OAc)(H$_2$O)$_2$](ClO$_4$)$_2\cdot$H$_2$O.

FIGURE 5 | χ_M vs. T, and χ_MT vs. T (insert) plots for [Co$_2$(L1)(μ-OAc)](ClO$_4$)$_2\cdot$0.5H$_2$O.

FIGURE 6 | **(A)** pH dependence profile, and **(B)** Michaelis-Menten plot for the hydrolysis of BDNPP catalyzed by [Ni$_2$(L1)(μ-OAc)(H$_2$O)$_2$](ClO$_4$)$_2\cdot$H$_2$O.

and **Figure 5** for [Co$_2$(L1)(μ-OAc)](ClO$_4$)$_2\cdot$0.5H$_2$O. For both complexes the susceptibility data were fitted using the program PHI (Chilton et al., 2013) with the isotropic exchange Hamiltonian $\hat{H} = -2J\hat{S}_1 \cdot \hat{S}_2$.

For [Ni$_2$(L1)(μ-OAc)(H$_2$O)$_2$](ClO$_4$)$_2\cdot$H$_2$O the χ_MT vs. T plot indicates antiferromagnetic coupling between the two Ni(II) centers, with χ_MT gradually decreasing from 3.63 cm^3 K mol^{-1} (μ_{eff} = 5.39 μ_B) at 300 K to 0.075 cm^3 K mol^{-1} (μ_{eff} = 0.77 μ_B) at 8 K. The room temperature value of χ_MT is larger than the spin-only value for two non-interacting high-spin nickel(II) ions (χ_MT = 2.00 cm^3 K mol^{-1}, μ_{SO} = 4.00 μ_B, g = 2.00, S = 1). While no orbital angular momentum is expected for the $^3A_{2g}$ ground state of the octahedral d^8 centers, it is expected for the excited $^3T_{2g}$ and $^3T_{1g}$ states. The theoretical χ_MT value with orbital angular momentum included is 4.99 cm^3 K mol^{-1} (μ_{SL} = 6.32 μ_B, L = 3), which suggests some orbital contributions are present in this case. The best fit gave parameters
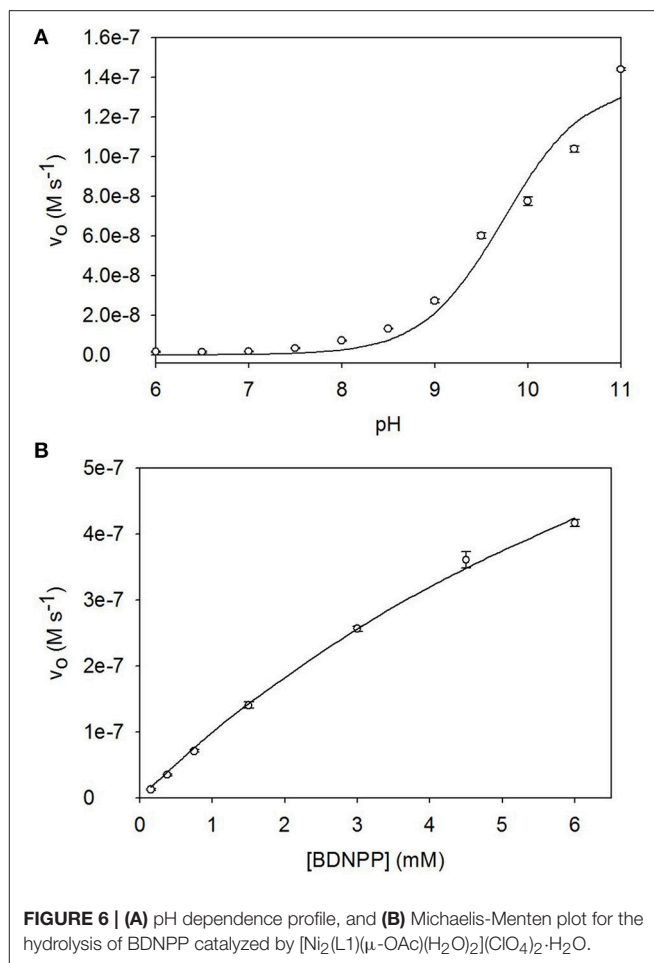
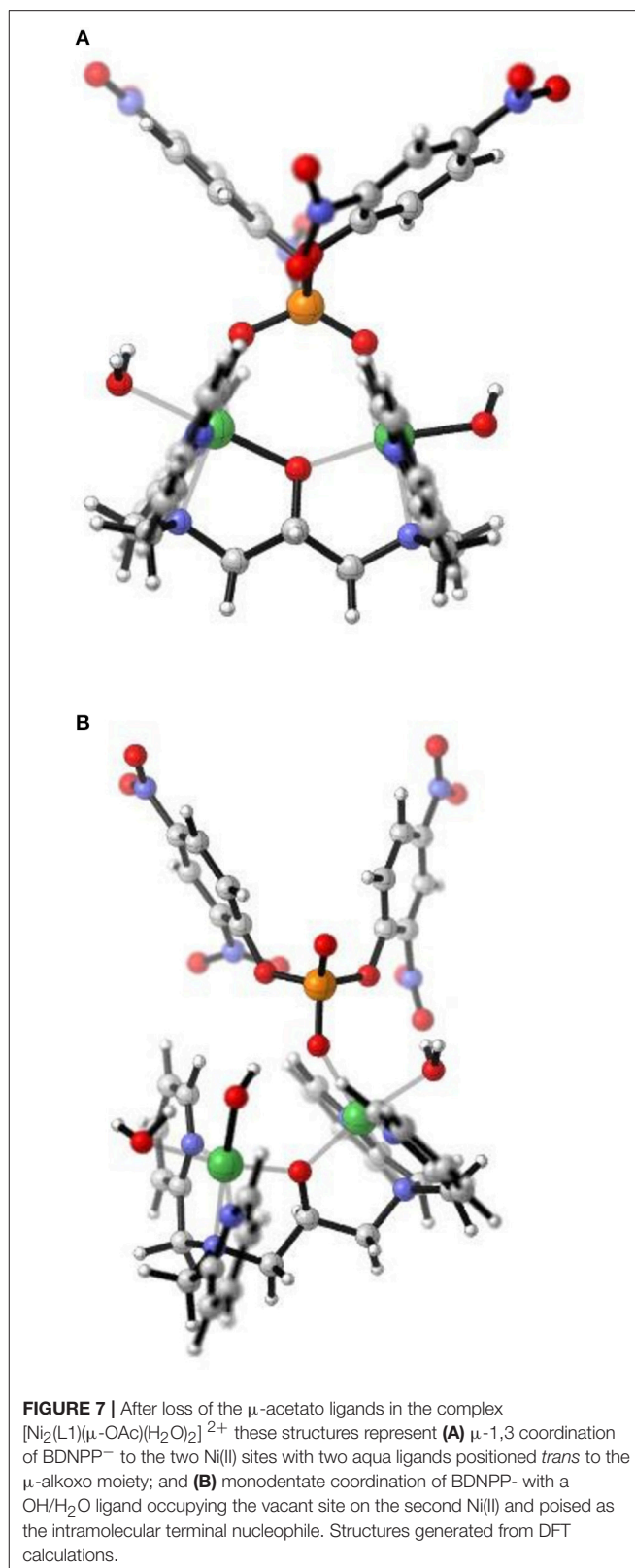J = -27.4 cm^{-1}, g = 2.29, D = 28.4 cm^{-1} and χ_{TIP} = 4.75 $\times$ 10^{-9} m^3 mol^{-1}. The inclusion of neither a rhombic zero-field splitting (ZFS) parameter E nor an intermolecular magnetic exchange parameter zJ led to an improvement of the fit and were thus omitted.

For [Co$_2$(L1)(μ-OAc)](ClO$_4$)$_2\cdot$0.5H$_2$O the magnetic moment has been reported as 4.09 μ_B/Co(II), measured in d$_3$-acetonitrile at room temperature (Siluvai and Murthy, 2009). In the study reported herein, the variable temperature magnetic susceptibility of the complex was measured from 300–7 K. The χ_MT value at 300 K is 4.23 cm^3 K mol^{-1} (μ_{eff} = 5.82 μ_B), which is within the range of similar binuclear cobalt(II) complexes (Zeng et al., 2004; Tian et al., 2007, 2008; Massoud et al., 2008; Jung et al., 2009; Daumann et al., 2013a; Khandar et al., 2015; Li et al., 2015; Alam et al., 2016). The value is higher than the expected spin-only value for two non-interacting high-spin cobalt(II) ions (3.74 cm^3 K mol^{-1}, μ_{SO} = 5.47 μ_B, g = 2.00, S = 3/2) but significantly lower than expected with the inclusion of orbital angular momentum (6.76 cm^3 K mol^{-1}, μ_{SL} = 7.35 μ_B, L = 3), suggesting only very minor orbital contributions. The value of χ_MT shows a gradual decrease with decreasing temperature and reaches 0.025 cm^3 K mol^{-1} at 7 K, indicative of antiferromagnetic coupling between the two centers. The best fit to the data gave parameters J = -14.9

cm^{-1}, $g = 2.16$ and $TIP = 2.22 \times 10^{-9}$ m^3 mol^{-1}. The inclusion of intermolecular magnetic exchange zJ was found to have little effect on the fit and, therefore, was not included. The fitted g value is larger than the free ion g value ($g_e = 2.00$) and is explained by second-order effects. While the $^4A_2'$ ground state arising from the trigonal bipyramidal coordination of a d^7 ion has no orbital angular momentum, admixture of the excited $^4E''$ state with the orbital angular momentum introduces second-order orbital momentum, resulting in a larger g value and magnetic moment (Hempel and Miller, 1981; Hossain and Sakiyama, 2002; Bai et al., 2005).

A computational study was undertaken employing the B3LYP functional, Noodleman's broken symmetry, the TZV basis set and the Orca set of programs (Noodleman et al., 1988; Schaefer et al., 1992; Becke, 1993; Neese, 2012; Frisch et al., 2013) in order to calculate the magnitude of the coupling in both complexes (Comba et al., 2009). The calculations were performed based on the X-ray structural parameters for the respective complexes. For the [Ni$_2$(L1)(μ-OAc)(H$_2$O)$_2$](ClO$_4$)$_2$·H$_2$O complex the computed value of $2J$ was similar to the experimentally determined value (−26.4 cm^{-1} compared with −27.4 cm^{-1}, respectively). For [Co$_2$(L1)(μ-OAc)](ClO$_4$)$_2$·0.5H$_2$O the difference in the calculated and experimental values was greater (−20.1 cm^{-1} compared with −14.9 cm^{-1}, respectively).

Attempts have been made to correlate structural parameters with the strength of coupling for both diNi(II) and diCo(II) complexes (Nanda et al., 1994a,b,c; Schultz et al., 1997; Johansson et al., 2008; Tomkowicz et al., 2012; Daumann et al., 2013b). In the case of diNi(II) complexes, an initial study reported a linear correlation between the magnitude and sign of J with the Ni-O-Ni angle for five diNi(II) complexes of the macrocyclic ligand 1^5,9^5-dimethyl-3,7,11,15-tetraaza-1,9(1,3)-dibenzenacyclohexadecaphane-1^2,9^2-diol, with aqua, thiocyanate, methanol, imidazole, and pyridine ligands completing the coordination sphere (Nanda et al., 1994c). The authors proposed that at an Ni-O-Ni angle of 97° a cross over from antiferro- to ferro-magnetic coupling occurred (Nanda et al., 1994c). The study was subsequently expanded to include examples of other diNi(II) complexes with phenoxido-bridged ligands and it was concluded that, with the availability of more structural data, a more definitive correlation between J and the Ni-O-Ni angle could be expected (Nanda et al., 1994a,b). In line with the previous analysis of the relationship between J and Ni-X bonds lengths it was suggested that, in hexacoordinate complexes, the antiferromagnetic coupling was amplified with an increase in bond lengths of one of the axial bonds (Nanda et al., 1994a). Further, the studies suggested that a significant increase in the magnitude of -J occurred in the situation where a tetragonally elongated hexacoordinate complex transformed to a five-coordinate square pyramidal complex (Nanda et al., 1994a). Subsequently, a series of studies reported and expanded on the correlations between the sign and magnitude of J and both the Ni-O-Ni and Ni-X bond lengths (Allen et al., 1978; Wages et al., 1993; Halcrow and Christou, 1994; Adams et al., 2001; Bu et al., 2001; Mochizuki et al., 2004; Prushan et al., 2007; Greatti et al., 2008; Pawlak et al., 2008; Mandal et al., 2009; Chattopadhyay

FIGURE 7 | After loss of the μ-acetato ligands in the complex [Ni$_2$(L1)(μ-OAc)(H$_2$O)$_2$]$^{2+}$ these structures represent **(A)** μ-1,3 coordination of BDNPP$^-$ to the two Ni(II) sites with two aqua ligands positioned *trans* to the μ-alkoxo moiety; and **(B)** monodentate coordination of BDNPP- with a OH/H$_2$O ligand occupying the vacant site on the second Ni(II) and poised as the intramolecular terminal nucleophile. Structures generated from DFT calculations.

et al., 2010; Ren et al., 2011; Biswas et al., 2012, 2017; Botana et al., 2014; Mahapatra et al., 2016; Massoud et al., 2016; Sanyal et al.,

**TABLE 3 |** Michaelis Menten kinetic data of dinuclear Ni(II) complexes that mimic metallophosphatases.

Ligand[a]	Complex	Substrate	Solvent	k_{cat} (s^{-1})	K_m (mM L^{-1})	References
2-[(4,7-diisopropyl-1,4,7-triazonan-1-yl)methyl]-4-methyl-6-[(pyridine-2-ylmethylamino)methyl]phenol (HL) (**1**)	[Ni$_2$(L)(μ-OAc)$_2$(OH$_2$)](BPh$_4$).H$_2$O	BDNPP	Acetonitrile/ aqueous buffer	0.013 (pH 9)	3.44	Xavier and Neves, 2016
2,6-bis[bis(2-pyridylmethyl)aminomethyl]-4-chlorophenol (HL^{ClO}) (**2**)	[Ni$_2$(L^{ClO})(μ-OAc)$_2$](PF$_6$).3H$_2$O	BDNPP	Acetonitrile/ aqueous buffer	2.80 × 10^{-3} (pH 7) 0.065 (pH 10.5)	0.21 (pH 7) 2.18 (pH 10.5)	Massoud et al., 2016
2-[(N-benzyl-N-2-pyridylmethylamine)]-4-methyl-6-[N-(2-pyridylmethyl)aminomethyl)])-4-methyl-6-formylphenol) (H$_2$BPPAMFF) (**3**)	[Ni$_2$(HBPPAMFF)(μ-OAc)$_2$(H$_2$O)](BPh$_4$)	BDNPP	Acetonitrile/ aqueous buffer	0.054 (pH 9)	1.57	Piovezan et al., 2012
2-[N-(2-(pyridyl-2-yl)ethyl)(1-methylimidazol-2-yl)aminomethyl]-4-methyl-6-[N-(2-(imidazol-4-yl)ethyl)aminomethyl]phenol (HL2) (**4**)	[Ni$_2$(L2)(μ-OAc)$_2$(CH$_3$CN)](BPh$_4$)	BDNPP	Acetonitrile/ aqueous buffer	0.034 (pH 9)	1.19	Greatti et al., 2008
2-[N-bis-(2-pyridylmethyl)aminomethyl]-4-methyl-6-[N-(2-pyridylmethyl)aminomethyl]phenol (HL$_A$1) (**5**)	[Ni$_2$(L$_A$1)(μ-OAc)$_2$(H$_2$O)]ClO$_4$.H$_2$O	BDNPP	Acetonitrile/ aqueous buffer	0.386 (pH 9)	5.67	Greatti et al., 2004, 2008
1,3-bis(bis(pyridin-2-ylmethyl)amino)propan-2-ol (HL^1) (**6**)	[Ni$_2$L^1(μ-OAc)(H$_2$O)$_2$](ClO$_4$)$_2$·H$_2$O	BDNPP	Acetonitrile/ aqueous buffer	~0.025 (pH 11)	10	This work
N-4-methyl-homopiperazine-N'-[N-(2-pyridylmethyl)-N-2-(2-pyridylethylamine)-1,3-diaminopropan-2-ol (HL) (**7**)	[Ni$_2$(L)(OH)]$^{2+}$	BNPP	Aqueous buffer	7.4 × 10^{-5} (pH 8.4)	6.95	Wu and Wang, 2014
2-[[(2-piperidylmethyl)amino]methyl]-4-bromo-6-[(1-methylhomopiperazine-4-yl)methyl]phenol (HL) (**8**)	[Ni$_2$(L)(OH)]$^{2+}$	BNPP	Ethanol/ aqueous buffer	1.49 × 10^{-4} (pH 8.3)	7.25	Ren et al., 2011
N,N,N',N'-tetrakis[(6-methyl-2-pyridyl)methyl]-1,3-diaminopropan-2-ol (Me$_4$tpdpH) (**9**)	[Ni$_2$(Me$_4$tpdp)(μ-OAc)$_2$(H$_2$O)] (ClO$_4$)	BNP	Acetonitrile/ aqueous buffer	k_{BNP} = 3.4 × 10^{-2} M^{-1} s^{-1}		Yamaguchi et al., 2001

[a] The numbers refer to the ligands shown in **Scheme 1**.

2016; Xavier and Neves, 2016). As the number of studies, and hence the number of examples of diNi(II) complexes with various bridging ligand types, has increased the relationship between J and a structural parameter (Ni-O-Ni angle; Ni-X distance) has been described in terms of both linear, albeit with considerable scatter (Mahapatra et al., 2016), and polynomial functions (Bu et al., 2001). Clearly, the relationship is dependent on a set of parameters and even on the type of bridging ligands (Krupskaya et al., 2010; Botana et al., 2014). The sign and magnitude of J (-27.4 cm^{-1}) for [Ni$_2$(L1)(μ-OAc)(H$_2$O)$_2$](ClO$_4$)$_2$·H$_2$O are consistent with the Ni^{II}-μO-Ni^{II} angle of 131.6(2)° (**Table S1** and **Figure S1**) (Nanda et al., 1994c; Mochizuki et al., 2004; Biswas et al., 2012, 2017; Massoud et al., 2016).

The relationship between the structural parameters and the magnitude of the observed magnetic coupling for dicobalt(II) complexes has been reviewed (Arora et al., 2012, p. 703; Tomkowicz et al., 2012; Daumann et al., 2013a). It was concluded that for complexes with a μ-O$_{bridge}$/bis(μ_2-RCOO-κ^2O:O') core, the variations in magnitude of J could be related to the type of μ-O$_{bridge}$, the Co-O$_{bridge}$-Co angle and the type of R-group (Tomkowicz et al., 2012). Further, it was proposed

that the strength of the coupling varied according to bridge type (μ-O^{2-}>μ-OH$^-$>μ-H$_2$O) (Schultz et al., 1997), and that Co(II)-O-Co(II) bond angles around 96° in some examples resulted in ferromagnetic coupling via orthogonal magnetic orbitals (Tudor et al., 2008; Fabelo et al., 2009; Tomkowicz et al., 2012), and it was also suggested that bis(μ_2-syn,syn-CH$_3$COO-κ^2O:O') bond angles were important (Arora et al., 2012). Extremely weak antiferro- or ferro-magnetic coupling was proposed for diCo(II) complexes with the μ-O$_{(phenoxido)}$;bis(μ_2-OAc-κ^2O:O') bridge, although exceptions occurred (Arora et al., 2012; Daumann et al., 2013a). Complexes with the μ-H$_2$O;bis(μ_2-RCOO-κ^2O:O') core appear to promote weak antiferromagnetic coupling, although stronger than that seen with the μ-O$_{(phenoxido)}$ analog; the bis(μ_2-RCOO-κ^2O:O');μ_2-O;κ^2O,O'-CH$_3$COO core appeared to promote ferromagnetic coupling (Daumann et al., 2013a). The relationship between Co(II)-X bond distances and the magnitude and sign of J was extremely weak, and both the Co(II)·Co(II) distance and extent of distortion around the Co(II) center seemingly having little bearing on the coupling (Daumann et al., 2013a). Of the structural parameters considered in this analysis, the
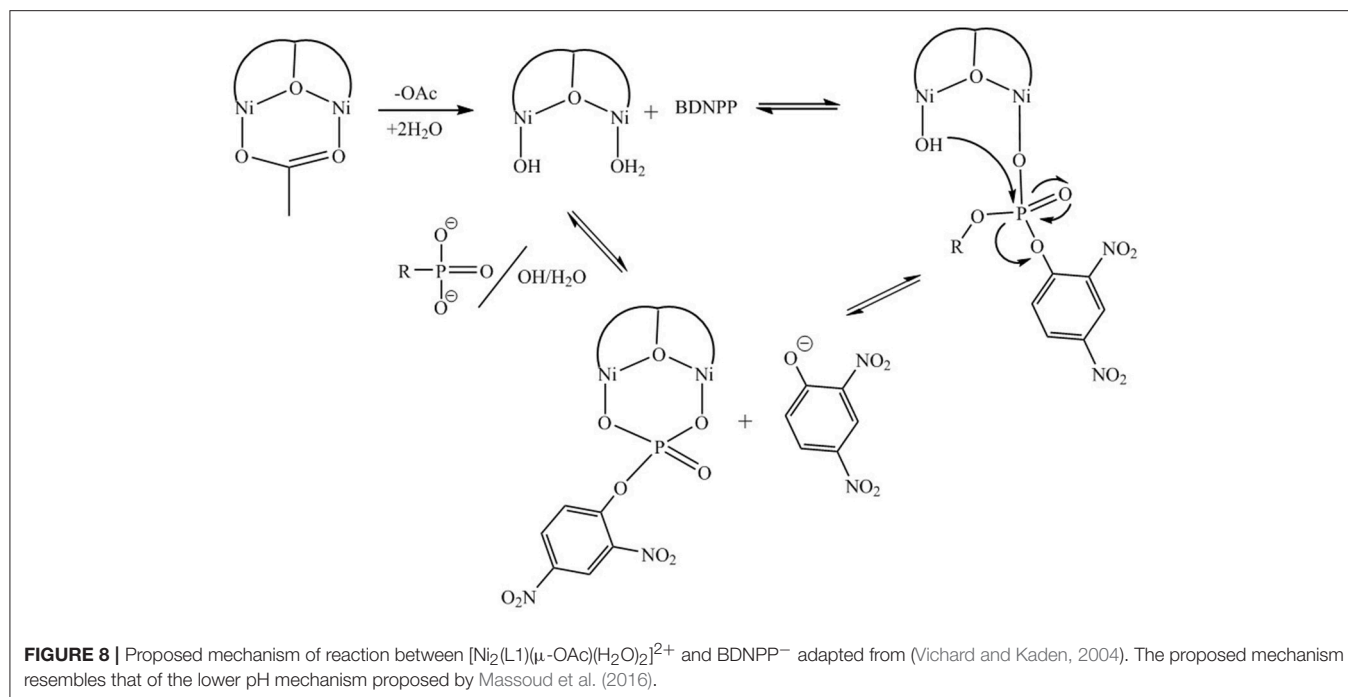
SCHEME 1 | The ligands listed in **Table 3**.
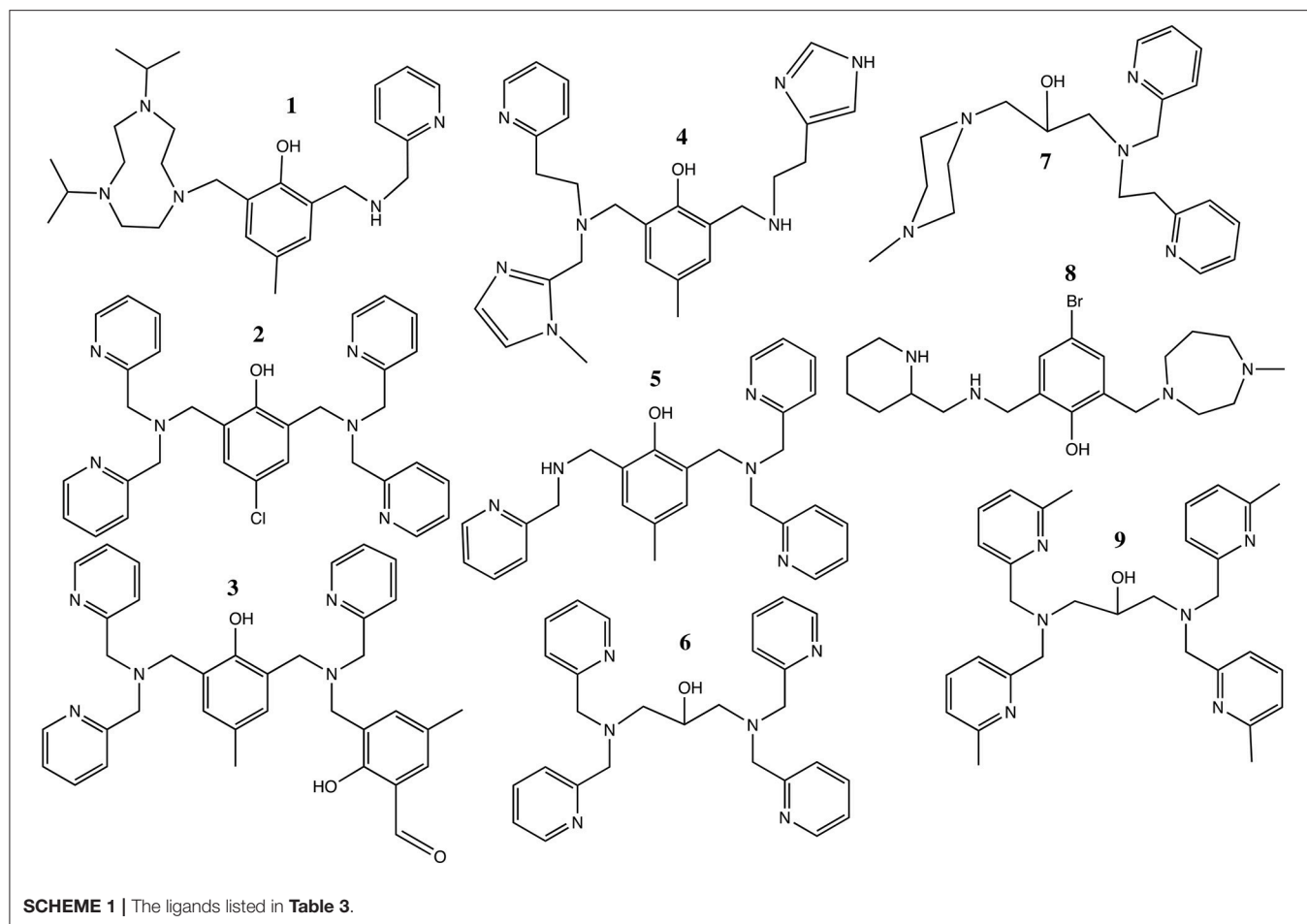
Co(II)-X-Co(II) bridge angles appear to have some influence on the sign and magnitude of J (Daumann et al., 2013a), in agreement with earlier studies, but none of the structural relationships appears to be particularly strong (**Table S2** and **Figure S2**; Johansson et al., 2008; Tudor et al., 2008; Fabelo et al., 2009; Tomkowicz et al., 2012).

Phosphoesterase Activity

The pH dependence of BDNPP hydrolysis by $[Ni_2(L1)(\mu\text{-}OAc)(H_2O)_2](ClO_4)_2 \cdot H_2O$ was analyzed between pH 4.75 and pH 11.0; the rate enhances sharply at pH values ≥ 9.0, reaching a maximum at pH ≥ 11.0. Data were fit as described in the Experimental section and resulted in an estimate of the pK_a value (9.7 ± 0.1) of the catalytically relevant protonation equilibrium (**Figure 6A**). Since the measurements of the catalytic rates as a function of [S] did not reach full saturation obtained catalytic parameters need to be viewed with some caution. A combination of non-linear and linear regression analyses indicate that plausible values for V_{max} and K_m are around $6–7 \times 10^{-5}$ M.min^{-1} and 10 mM, respectively (**Figure 6B**). For the following comparison of the catalytic efficiencies of a number of Ni-dependent biomimetics we will use the rate of hydrolysis of 6 mM [S] by 40 μM $[Ni_2(L1)(OAc)(H_2O)_2](ClO_4)_2 \cdot H_2O$, i.e., 2.50×10^{-5} M.min^{-1}. This rate corresponds to a k_{cat} of ~0.01 s^{-1}.

Several previous studies focused on the phosphatase-like activity of di-Ni(II) complexes (**Table 3** and **Scheme 1**; Yamaguchi et al., 1997, 2001; Yamane et al., 1997, 2001; Parimala and Kandaswamy, 2003; Jikido et al., 2005; Greatti et al., 2008; Ren et al., 2011; Piovezan et al., 2012; Wu and Wang, 2014; Massoud et al., 2016; Xavier and Neves, 2016). In a number of cases the experimental conditions in terms of solvent (acetonitrile/aqueous buffer) and substrate (BDNPP) were similar to those employed in the present work, although the pH at which the k_{cat} and K_m values were determined did vary, making direct comparisons difficult (Greatti et al., 2004, 2008; Piovezan et al., 2012; Massoud et al., 2016; Xavier and Neves, 2016). The nucleophilic agent in these reactions has been proposed as either a terminal (Yamaguchi et al., 2001; Vichard and Kaden, 2002; Parimala and Kandaswamy, 2003; Jikido et al., 2005; Greatti et al., 2008; Massoud et al., 2016; Sanyal et al., 2016) or a bridging (Ren et al., 2011; Piovezan et al., 2012; Wu and Wang, 2014) hydroxido moiety.

Of the examples listed in **Table 3**, the complex with the ligand 2-[N-bis-(2-pyridylmethyl)aminomethyl]-4-methyl-6-[N-(2-pyridylmethyl)aminomethyl]phenol, $[Ni_2(L_A1)(\mu\text{-}OAc)_2(H_2O)]ClO_4 \cdot H_2O$, was the most effective and efficient catalyst for the hydrolysis of BDNPP with $k_{cat} = 0.386$ s^{-1} at pH 9 (Greatti et al., 2008). The rate enhancement was rationalized

FIGURE 8 | Proposed mechanism of reaction between $[Ni_2(L1)(\mu\text{-}OAc)(H_2O)_2]^{2+}$ and $BDNPP^-$ adapted from (Vichard and Kaden, 2004). The proposed mechanism resembles that of the lower pH mechanism proposed by Massoud et al. (2016).

in terms of the fact that in solution at pH 9.00, the active species $[Ni_2(L_A1)(H_2O)_2(\mu\text{-}OH)]^{2+}$ made up approximately 85% of the complexes present in solution (Greatti et al., 2008). The proposed mechanism for the reaction involved initial loss of the bridging acetate ligands and coordination of BDNPP after replacement of one aqua ligand (Greatti et al., 2008). The substrate is thus proposed to coordinate in a monodentate manner and orient *cis* to a terminal Ni-OH moiety, the latter promoting a nucleophilic attack on the phosphorus atom with release of the nitrophenolate anion and formation of a bridging DNP molecule. A subsequent intramolecular nucleophilic attack by a μ-OH moiety on the μ-DNP was proposed to result in loss of a second nitrophenolate anion and formation of coordinated phosphate anion which was subsequently replaced by H_2O/OH^- to complete the cycle (Greatti et al., 2008). In the case of the complex $[Ni_2(Me_4tpdp)(\mu\text{-}OAc)_2(H_2O)](ClO_4)$, a mechanism was proposed whereby the substrate, bis(4-nitrophenyl)phosphate (BNP) was coordinated in a μ-1,3 manner to the diNi(II) complex, after loss of the acetate ligands, with subsequent nucleophilic attack by a terminal Ni-OH moiety at the phosphorus center (Yamaguchi et al., 2001). In that case the reaction is facilitated by the fact that the relevant hydroxido ligand is arranged *cis*, and thus adjacent, to the substrate (Yamaguchi et al., 2001). A variation of the above mechanisms was proposed for $[Ni_2(L^{Cl}O)(\mu\text{-}OAc)_2](PF_6)\cdot3H_2O$ by Massoud et al.; in the initial phase of the catalytic cycle one of two metal-bridging acetate groups is displaced and the substrate BDNPP binds to one of the Ni(II). Subsequently, dependent on pH, the attack of a terminal hydroxide that either resides on the same (high pH) or the opposite (low pH) metal as the substrate attacks the phosphorus moiety, leading to the DNPP product being coordinated either bidentately to one metal or to both metals, respectively (Massoud et al., 2016).

For $[Ni_2(L1)(\mu\text{-}OAc)(H_2O)_2](ClO_4)_2\cdot H_2O$ both Ni(II) sites are six-coordinate. Loss of the μ-acetato ligand is thus a prerequisite for catalytic activity as it generates vacant positions for the substrate to bind (**Figure 7A**). However, according to the crystal structure (**Figure 2**) none of the available aqua/hydroxido ligands are positioned suitably to act as nucleophiles for the reaction. We thus propose that the release of the μ-acetato group enables the monodentate coordination of the substrate to one of the Ni(II) ions and a water molecule (with a pK_a of ∼9.7) to the other metal ion (**Figure 7B**). The subsequent attack by the deprotonated water ligand on the phosphorus moiety of the substrate triggers catalysis (**Figure 8**). Insofar, the model resembles that of the lower pH mechanism proposed by Massoud et al. (2016). In the latter complex the presence of two metal-bridging acetate groups provides the basis for an enhanced mechanistic flexibility (i.e., low and high pH pathways), where the nucleophile can be either bound to the same or the opposite metal ion as the substrate.

The phosphatase-like activity of the analogous $[Co_2L1(\mu\text{-}OAc)](ClO_4)_2\cdot0.5\cdot H_2O$ could not be investigated under corresponding experimental conditions since the initially red colored solution turned yellow after the addition of the aqueous buffer solution. The absorbance of the mixture at 400 nm increased upon standing, making any attempt to measure the formation of the dinitrophenolate anion difficult. The change of color of the solution may be explained by the oxidation of cobalt(II) ions (Suzuki et al., 1990).

CONCLUSIONS

The dinickel(II) and dicobalt(II) complexes of 1,3-bis(bis(pyridin-2-ylmethyl)amino)propan-2-ol have been

prepared and some of their properties were compared. Magnetic susceptibility studies confirmed that the two metal ions in both complexes are antiferromagnetically coupled and computational studies verified the experimental magnetic coupling constants. Attempted correlation of the relationship between structural parameters, particularly the M-O-M angles, with the strength of the magnetic coupling were only partially successful. Kinetic analysis with the activated substrate BDNPP suggested that for the diNi(II) complex a terminal water is the nucleophile with a kinetically relevant pK_a of 9.7 ± 0.1 and a k_{cat} value as high as $0.025 \ s^{-1}$ (**Table 3**). The complex is thus at the higher end of the range for catalytic efficiency for similar diNi(II) complexes with this substrate (the corresponding diCo(II) complex was found to oxidize readily in the buffer solution). Thus, although no suitable nucleophile (OH^-) is present in the original molecule the replacement of the two acetate bridges by water and/or substrate molecules (**Figure 8**) may not be rate-limiting. The complex is proposed to employ a similar mechanism as proposed for a series of analogous model systems for enzymes such as PAPs (Smith et al., 2009; Comba et al., 2012a,b; Bernhardt et al., 2015; Roberts et al., 2015; Bosch et al., 2016). The majority of complexes listed in **Table 3** attain optimal catalytic efficiency under alkaline conditions (>pH 9.0), somewhat higher than the pH optimum of the di-Ni(II) enzyme urease (pH 7.4). This difference may be due to the fact that the majority of model systems use a terminally bound nucleophile to initiate the hydrolytic reaction, whereas urease employs a metal ion-bridging hydroxide (Zambelli et al., 2011). Nonetheless, it is apparent that the complexes listed in **Table 3** represent suitable functional models for biological catalysts such as ureases and PAPs.

AUTHOR CONTRIBUTIONS

AH designed the project and supervised the synthetic chemistry and hydrolytic experiments, contributed to the writing of the manuscript. DE undertook the syntheses of the ligand and the metal complex and undertook the spectroscopic characterization. AR undertook the magnetochemical study and analyzed the results. PC in association with AR supervised the magnetochemical study and data analysis. GS contributed to the design of the project, supplied the funding for the work, and contributed to the writing of the manuscript. EK contributed to the writing of the DFT section of the manuscript and assisted with DFT calculations. LG undertook the X-ray structure analysis, contributed to the analysis of the kinetic data, undertook the DFT studies, and contributed to the writing of the manuscript.

ACKNOWLEDGMENTS

SUPPLEMENTARY MATERIAL

The Supplementary Material for this article can be found online at: https://www.frontiersin.org/articles/10.3389/fchem.2018.00441/full#supplementary-material

REFERENCES

Adams, H., Bradshaw, D., and Fenton, D., E. (2001). Dinuclear nickel(II) and zinc(II) complexes of 2,6-[N,N'-bis(2-hydroxyphenylmethyl)-N,N'-bis(2-pyridylmethyl)aminomethyl]-4-methyl-phenol. *Supramol. Chem.* 13, 513–519. doi: 10.1080/10610270108028297

Addison, A. W., Rao, T. N., Reedijk, J., Van Rijn, J., and Verschoor, G. C. (1984). Synthesis, structure, and spectroscopic properties of copper(II) compounds containing nitrogen-sulfur donor ligands: the crystal and molecular structure of aqua[1,7-bis(N-methylbenzimidazol-2'-yl)-2,6-dithiaheptane]copper(II) perchlorate. *J. Chem. Soc. Dalton Trans.* 1349–1356. doi: 10.1039/DT9840001349

Alam, R., Pal, K., Shaw, B. K., Dolai, M., Pal, N., and Ali, M. (2016). Synthesis, structure, catalytic and magnetic properties of a pyrazole based five coordinated di-nuclear cobalt(II) complex. *Polyhedron* 106, 84–91. doi: 10.1016/j.poly.2015.12.062

Allen, K. G., Stewart, J. A., Johnson, P. E., and Wettlaufer, D. G. (1978). Identification of the ionic groups of papain by pH/rate profile analysis. *Eur. J. Biochem.* 87, 575–582. doi: 10.1111/j.1432-1033.1978.tb12409.x

Arora, H., Barman, S. K., Lloret, F., and Mukherjee, R. (2012). Isostructural dinuclear phenoxo/acetato bridged mangnaese(II), cobalt(II) and zinc(II)

complexes with labile sites: kinetics of transesterification of 2-hydroxypropyl-p-nitrophenylphosphate. *Inorg. Chem.* 51, 5539–5553. doi: 10.1021/ic201971t

Ashwini, K. (2006). Importance of elements in daily life. *J. Teach. Res. Chem.* 13, 86–89.

Bai, S.-Q., Gao, E.-Q., He, Z., Fang, C.-J., and Yan, C.-H. (2005). Crystal structures and magnetic behavior of three new azido-bridged dinuclear cobalt(II) and copper(II) complexes. *New J. Chem.* 29, 935–941. doi: 10.1039/b418239a

Bain, G. A., and Berry, J. F. (2008). Diamagnetic corrections and Pascal's constants. *J. Chem. Educ.* 85, 532–536. doi: 10.1021/ed085p532

Barondeau, D. P., Kassmann, C. J., Bruns, C. K., Tainer, J. A., and Getzoff, E. D. (2004). Nickel superoxide dismutase structure and mechanism. *Biochemistry* 43, 8038–8047. doi: 10.1021/bi0496081

Becke, A. D. (1993). Density-functional thermochemistry. III. the role of exact exchange. *J. Chem. Phys.* 98, 5648–5652. doi: 10.1063/1.464913

Bernhardt, P. V., Bosch, S., Comba, P., Gahan, L. R., Hanson, G. R., Wadepohl, H., et al. (2015). An approach to more accurate model systems for purple acid phosphatases (PAPs). *Inorg. Chem.* 54, 7249–7263. doi: 10.1021/acs.inorgchem.5b00628

Bernhardt, P. V., Schenk, G., and Wilson, G. J. (2004). Direct electrochemistry of porcine purple acid phosphatase (Uteroferrin). *Biochemistry* 43: 10387–10392. doi: 10.1021/bi0490338

Biswas, A., Das, L. K., Drew, M. G., Aromí, G., Gamez, P., and Ghosh, A. (2012). Synthesis, crystal structures, magnetic properties and catecholase activity of

double phenoxido-bridged penta-coordinated dinuclear nickel(II) complexes derived from reduced schiff-base ligands: mechanistic inference of catecholase activity. *Inorg. Chem.* 51, 7993–8001. doi: 10.1021/ic202748m

Biswas, A., Drew, M. G. B., Gomez-Garcia, C. J., and Ghosh, A. (2017). Formation of a dinuclear and a trinuclear Ni(II) complex on slight variation of experimental conditions: Structural analysis and magnetic properties. *Polyhedron* 121, 80–87. doi: 10.1016/j.poly.2016.09.050

Blakeley, R. L., Treston, A., Andrews, R. K., and Zerner, B. (1982). Nickel(II)-promoted ethanolysis and hydrolysis of N-(2-pyridylmethyl)urea. a model for urease. *J. Am. Chem. Soc.* 104, 612–614. doi: 10.1021/ja00366a040

Blakeley, R. L., and Zerner, B. (1984). Jack bean urease: the first nickel enzyme. *J. Mol. Catal.* 23, 263–292. doi: 10.1016/0304-5102(84)80014-0

Bosch, S., Comba, P., Gahan, L. R., and Schenk, G. (2016). *Asymmetric mono- and dinuclear GaIII and ZnII complexes as models for purple acid phosphatases*. *J. Inorg. Biochem.* 162, 343–355. doi: 10.1016/j.jinorgbio.2015.12.028

Botana, L., Ruiz, J., Mota, A. J., Rodriguez-Dieguez, A., Seco, J. M., Colacio, E., et al. (2014). Anion controlled structural and magnetic diversity in unusual mixed-bridged polynuclear NiII complexes with a versatile bis(2-methoxy phenol)diamine hexadentate ligand. an experimental and theoretical magneto-structural study. *Dalton Trans.* 43, 13509–13524. doi: 10.1039/C4DT01253D

Bu, X.-H., Du, M., Zhang, L., Liao, D.-Z., Tang, J.-K., Shionoya, R.-M., et al. (2001). Novel nickel(II) complexes with diazamesocyclic ligands functionalized by additional phenol donor pendant(s): synthesis, characterization, crystal structures and magnetic properties. *J. Chem. Soc. Dalton Trans.* 593–598. doi: 10.1039/b008297j

Chattopadhyay, T., Mukherjee, M., Mondal, A., Maiti, P., Banerjee, A., Banu, K., et al. (2010). A unique nickel system having versatile catalytic activity of biological significance. *Inorg. Chem.* 49, 3121–3129. doi: 10.1021/ic901546t

Chilton, N. F., Anderson, R. P., Turner, L. D., Soncini, A., and Murray, K. S. (2013). PHI: a powerful new program for the analysis of anisotropic monomeric and exchange-coupled polynuclear d- and f-block complexes. *J. Comput. Chem.* 34, 1164–1175. doi: 10.1002/jcc.23234

Comba, P., Gahan, L. R., Hanson, G. R., Mereacre, V., Noble, C. J., Powell, A. K., et al. (2012a). Monoesterase activity of a purple acid phosphatase mimic with a cyclam platform. *Chem. Eur. J.* 18, 1700–1710. doi: 10.1002/chem.201100229

Comba, P., Gahan, L. R., Mereacre, V., Hanson, G. R., Powell, A. K., Schenk, G., et al. (2012b). Spectroscopic characterization of the active FeIIIFeIII and FeIIIFeII forms of a purple acid phosphatase model system. *Inorg. Chem.* 51, 12195–12209. doi: 10.1021/ic301347t

Comba, P., Hausberg, S., and Martin, B. (2009). Calculation of exchange coupling constants of transition metal complexes with DFT. *J. Phys. Chem. A* 113, 6751–6755. doi: 10.1021/jp900752p

Daumann, L. J., Comba, P., Larrabee, J. A., Schenk, G., Stranger, R., Gahan, L. R. et al. (2013a). Synthesis, magnetic properties, and phosphoesterase activity of dinuclear cobalt(II) complexes. *Inorg. Chem.* 52, 2029–2043. doi: 10.1021/ic302418x

Daumann, L. J., Larrabee, J. A., Comba, P., Schenk, G., and Gahan, L. R. (2013b). Dinuclear cobalt(II) complexes as metallo-β-lactamase mimics. *Eur. J. Inorg. Chem.* 3082–3089. doi: 10.1002/ejic.201300280

Deacon, G. B., and Phillips, R. J. (1980). Relationships between the carbon-oxygen stretching frequencies of carboxylato complexes and the type of carboxylate coordination. *Coord. Chem. Rev.* 33, 227–250. doi: 10.1016/S0010-8545(00)80455-5

Dixon, N. E., Gazzola, C., Asher, C. J., Lee, D. S., Blakeley, R. L., and Zerner, B. (1980). Jack been urease (EC 3.5.1.5). II. the relationship between nickel, enzymatic activity, and the "abnormal" ultraviolet spectrum. the nickel content of jack beans. *Can. J. Biochem.* 58, 474–480. doi: 10.1139/o80-063

Ensign, S. A., Bonam, D., and Ludden, P. W. (1989). Nickel is required for the transfer of electrons from carbon monoxide to the iron-sulfur center(s) of carbon monoxide dehydrogenase from Rhodospirillum rubrum. *Biochemistry* 28, 4968–4973. doi: 10.1021/bi00438a010

Ensign, S. A., Campbell, M. J., and Ludden, P. W. (1990). Activation of the nickel-deficient carbon monoxide dehydrogenase from *Rhodospirillum rubrum*: kinetic characterization and reductant requirement. *Biochemistry* 29, 2162–2168. doi: 10.1021/bi00460a029

Fabelo, O., Cañadillas-Delgado, L., Pasán, J., Delgado, F. S., Lloret, F., Ruiz-Perez, C., et al. (2009). Study of the influence of the bridge on the magnetic coupling in cobalt(II) complexes. *Inorg. Chem.* 48, 11342–11351. doi: 10.1021/ic901843r

Farrugia, L. J. (1999). WinGX suite for small-molecule single-crystal crystallography. *J. Appl. Crystallogr.* 32, 837–838. doi: 10.1107/S0021889899006020

Flanagan, J. U., Cassady, A. I., Schenk, G., Guddat, L. W., and Hume, D. A. (2006). Identification and molecular modelling of a novel, plant-like, human purple acid phosphatase. *Gene* 377, 12–20. doi: 10.1016/j.gene.2006.02.031

Frisch, M. J., Trucks, G. W., Schlegel, H. B., Scuseria, G. E., Robb, M. A., Fox, D. J., et al. (2013). *Gaussian 09, Revision D.01*. Wallingford CT: Gaussian, Inc.

Gencic, S., and Grahame, D. A. (2003). Nickel in subunit beta of the acetyl-CoA decarbonylase/synthase multienzyme complex in methanogens. catalytic properties and evidence for a binuclear Ni-Ni site. *J. Biol. Chem.* 278, 6101–6110. doi: 10.1074/jbc.M210484200

Greatti, A., Scarpellini, M., Peralta, R. A., Casellato, A., Bortoluzzi, A. J., Xavier, F. R., et al. (2008). Synthesis, structure, and physicochemical properties of dinuclear NiII complexes as highly efficient functional models of phosphohydrolases. *Inorg. Chem.* 47, 1107–1119. doi: 10.1021/ic702132t

Greatti, A. M., Aires de Brito, Bortoluzzi, A. J., and Ceccato, A. S. (2004). Synthesis, characterization and structure of a new dinickel(II) complex as model for urease. *J. Mol. Struct.* 688, 185–190. doi: 10.1016/j.molstruc.2003.10.008

Halcrow, M. A., and Christou, G. (1994). Biomimetic chemistry of nickel. *Chem. Rev.* 94, 2421–2481. doi: 10.1021/cr00032a008

Hempel, J. C., and Miller, M. E. (1981). Ground state properties of trigonal prismatic and trigonal bipyramidal d1,9, d2,8, d3,7, and d5 systems: effects of trigonal distortion. *J. Chem. Phys.* 75, 2959–2970. doi: 10.1063/1.442387

Hossain, M. J., and Sakiyama, H. (2002). Two typical cases of magnetism for dinuclear high-spin cobalt(II) complexes in trigonal-bipyramidal fields. *Inorg. Chim. Acta* 338, 255–259. doi: 10.1016/S0020-1693(02)01053-8

Jacoby, M. (1933). The action of metals on enzymes. *Biochem. Z* 259, 211–222.

Jikido, R., Shiraishi, H., Matsufuji, K., Ohba, M., Furutachi, H., Suzuki, M., et al. (2005). Mass spectrometric and spectroscopic studies on hydrolysis of phosphoesters by bis(μ-acetato)-μ-phenolato dinuclear metal(II) complexes (metal = Mn, Co, Ni, and Zn). *Bull. Chem. Soc. Jpn.* 78, 1795–1803. doi: 10.1246/bcsj.78.1795

Johansson, F. B., Bond, A. D., Nielsen, U. G., Moubaraki, B., Murray, K., S., McKenzie, C. J. et al. (2008). Dicobalt II-II, II-III, and III-III complexes as spectroscopic models for dicobalt enzyme active sites. *Inorg. Chem.* 47, 5079–5092. doi: 10.1021/ic7020534

Jung, M., Sharma, A., Hinderberger, D., Braun, S., Schatzschneider, U., and Rentschler, E. (2009). Nitronyl nitroxide radicals linked to exchange-coupled metal dimers - studies using X-ray crystallography, magnetic susceptibility measurements, EPR spectroscopy, and DFT calculations. *Eur. J. Inorg. Chem.* 1495–1502. doi: 10.1002/ejic.200801248

Kaminskaia, N. V., Spingler, B., and Lippard, S., J. (2000). Hydrolysis of β-lactam antibiotics catalyzed by dinuclear zinc(II) complexes: functional mimics of metallo-β-lactamases. *J. Am. Chem. Soc.* 122, 6411–6422. doi: 10.1021/ja993704l

Kantacha, A., Buchholz, R., Smith, S. J., Schenk, G., and Gahan, L. R. (2011). Phosphate ester cleavage promoted by a tetrameric iron(III) complex. *J. Biol. Inorg. Chem.* 16, 25–32. doi: 10.1007/s00775-010-0696-0

Khandar, A. A., Kirschbaum, K., Abedi, M., Mock, K., Tracy, G., Spasojevic, V., et al. (2015). Synthesis, characterization and crystal structures of mono and dinuclear macrocyclic cobalt(II) complexes with a new tetraaza m-xylyl-based macrocyclic ligand. *New J. Chem.* 39, 2822–2831. doi: 10.1039/C4NJ01608D

Krupskaya, Y., Alfonsov, A., Parameswaran, A., Kataev, V., Klingeler, R., Steinfeld, G., et al. (2010). Interplay of magnetic exchange interactions and Ni-S-Ni bond angles in polynuclear nickel(II) complexes. *ChemPhysChem* 11, 1961–1970. doi: 10.1002/cphc.200900935

Li, J.-L., Jiang, L., Wang, B.-W., Tian, J.-L., Gu, W., Yan, P., et al. (2015). Bio-relevant cobalt(II) complexes with compartmental polyquinoline ligand: synthesis, crystal structures and biological activities. *J. Inorg. Biochem.* 145, 19–29. doi: 10.1016/j.jinorgbio.2014.11.003

Mahapatra, P., Ghosh, S., Giri, S., and Ghosh, A. (2016). The unusual intermediate species in the formation of Ni(II) complexes of unsymmetrical Schiff bases by Elder's method: structural, electrochemical and magnetic

characterizations. *Polyhedron* 117, 427–436. doi: 10.1016/j.poly.2016.06.020

Mandal, S., Balamurugan, V., Lloret, F., and Mukherjee, R. (2009). Syntheses, X-ray structures, and physicochemical properties of phenoxo-bridged dinuclear nickel(II) complexes: kinetics of transesterification of 2-hydroxypropyl-p-nitrophenyl phosphate. *Inorg. Chem.* 48, 7544–7556. doi: 10.1021/ic8018937

Massoud, S. S., Broussard, K. T., Mautner, F. A., Vicente, R., Saha, M. K., and Bernal, I. (2008). Five-coordinate cobalt(II) complexes of tris(2-pyridylmethyl)amine (TPA): synthesis, structural and magnetic characterization of a terephthalato-bridged dinuclear cobalt(II) complex. *Inorg. Chim. Acta* 361, 123–131. doi: 10.1016/j.ica.2007.06.021

Massoud, S. S., Ledet, C. C., Junk, T., Bosch, S., Comba, P., Mautner, F. A., et al. (2016). Dinuclear metal(II)-acetato complexes based on bicompartmental 4-chlorophenolate: syntheses, structures, magnetic properties, DNA interactions and phosphodiester hydrolysis. *Dalton Trans.* 45, 12933–12950. doi: 10.1039/C6DT02596J

Mendes, L. L., Englert, D., Fernandes, C., Gahan, L. R., Schenk, G., and Horn, A. (2016). Metallohydrolase biomimetics with catalytic and structural flexibility. *Dalton Trans.* 45, 18510–18521. doi: 10.1039/C6DT03200A

Meyer, F. (2009). Synthetic models for the urease active site. *Prog. Inorg. Chem.* 56, 487–542. doi: 10.1002/9780470440124.ch6

Mitić, N., Hadler, K. S., Gahan, L. R., Hengge, A. C., and Schenk, G. (2010). The divalent metal ion in the active site of uteroferrin modulates substrate binding and catalysis. *J. Am. Chem. Soc.* 132, 7049–7054. doi: 10.1021/ja910583y

Mitić, N., Noble, C. J., Gahan, L. R., Hanson, G. R., and Schenk, G. (2009). Metal ion mutagenesis – conversion of a purple acid phosphatase from sweet potato to a neutral phosphatase with the formation of an unprecedented catalytically competent $Mn^{II}Mn^{II}$ active site. *J. Am. Chem. Soc.* 131, 8173–8179. doi: 10.1021/ja900797u

Mochizuki, K., Hasegawa, A., and Weyhermuller, T. (2004). Synthesis, structures, and magnetic properties of dicopper(II) and dinickel(II) complexes with a new bis(macrocycle), 7,7'-(2-hydroxypropane-1,3-diyl)bis{3,7,11,17-tetraazabicyclo[11.3.1]- heptadeca-1(17),13,15-triene}. *Inorg. Chim. Acta* 357, 3245–3250. doi: 10.1016/j.ica.2004.01.047

Moffat, C. D., Weiss, D. J., Shivalingam, A., White, A. J., Salaün, P., and Vilar, R. (2014). Molecular recognition and scavenging of arsenate from aqueous solution using dimetallic receptors. *Chem. Eur. J.* 20, 17168–17177. doi: 10.1002/chem.201404723

Nanda, K. K., Das, R., Thompson, L., K., Venkatsubramanian, K., Paul, P., and Nag, K. (1994b). Magneto-structural correlations in macrocyclic dinickel(II) complexes: tuning of spin exchange by varying stereochemistry and auxiliary ligands. *Inorg. Chem.* 33, 1188–1193. doi: 10.1021/ic00084a036

Nanda, K. K., Das, R., Thompson, L. K., Venkatsubramanian, K., and Nag, K. (1994a). Combined Effect of phenoxy and carboxylate bridges on magnetic properties of a series of macrocyclic dinickel(II) complexes. *Inorg. Chem.* 33, 5934–5939. doi: 10.1021/ic00103a048

Nanda, K. K., Thompson, L., K., Bridson, J., N., and Nag, K. (1994c). Linear dependence of spin exchange coupling constant on bridge angle in phenoxy-bridged dinickel(II) complexes. *J. Chem. Soc. Chem. Commun.* 1337–1338. doi: 10.1039/c39940001337

Neese, F. (2012). The ORCA program system. wiley Interdiscip. *Rev. Comput. Mol. Sci.* 2, 73–78. doi: 10.1002/wcms.81

Noodleman, L., Case, D. A., and Aizman, A. (1988). Broken symmetry analysis of spin coupling in iron-sulfur clusters. *J. Am. Chem. Soc.* 110, 1001–1005. doi: 10.1021/ja00212a003

Parimala, S., and Kandaswamy, M. (2003). Mononuclear, dinuclear nickel(II) and heterodinuclear Zn(II)Ni(II) complexes as models for the active site of phosphatase. *Inorg. Chem. Commun.* 6, 1252–1254. doi: 10.1016/S1387-7003(03)00243-0

Pawlak, P. L., Malkhasian, A. Y. S., Sjlivic, B., Tiza, M. J., Kucera, B. E., Chavez, F. A., et al. (2008). Synthesis, structure, and magnetic properties of a new binuclear Ni(II) complex supported by 1,4,8-triazacycloundecane. *Inorg. Chem. Commun.* 11, 1023–1026. doi: 10.1016/j.inoche.2008.05.014

Piovezan, C., Silva, J. M. R., Neves, A., Bortoluzzi, A. J., Haase, W., Rossi, L. M., et al. (2012). Design of a dinuclear nickel(II) bioinspired hydrolase to bind covalently to silica surfaces: synthesis, magnetism, and reactivity studies. *Inorg. Chem.* 51, 6104–6115. doi: 10.1021/ic300018t

Prushan, M. J., Tomezsko, D. M., Lofland, S., Zeller, M., and Hunter, A. D. (2007). A nickel(II) di-µ2-phenolato bridged dinuclear complex: weak antiferromagnetic interactions in nickel(II) dimers. *Inorg. Chim. Acta* 360, 2245–2254. doi: 10.1016/j.ica.2006.11.008

Przybyla, A. E., Robbins, J., Menon, N., and Peck, H. D. Jr (1992). Structure-function relationships among the nickel-containing hydrogenases. *FEMS Microbiol. Rev.* 8, 109–135. doi: 10.1111/j.1574-6968.1992.tb04960.x

Ren, Y.-W., Lu, J.-X., Cai, B.-W., Shi, D.-B., Jiang, H.-F., Chen, J., et al. (2011). A novel asymmetric di-Ni(II) system as a highly efficient functional model for phosphodiesterase: synthesis, structures, physicochemical properties and catalytic kinetics. *Dalton Trans.* 40, 1372–1381. doi: 10.1039/C0DT01194K

Roberts, A. E., Schenk, G., and Gahan, L. R. (2015). A heterodinuclear FeIIIZnII complex as a mimic for purple acid phosphatase with site-specific ZnII binding. *Eur. J. Inorg. Chem.* 2015, 3076–3086. doi: 10.1002/ejic.201500351

Sanyal, R., Zhang, X., Chakraborty, P., Giri, S., Chattopadhyay, S. K., Das, D. et al. (2016). Role of solvent in the phosphatase activity of a dinuclear nickel(II) complex of a Schiff base ligand: mechanistic interpretation by DFT studies. *New J. Chem.* 40, 7388–7398. doi: 10.1039/C6NJ01043A

Sargent, F. (2016). The Model [NiFe]-hydrogenases of *escherichia coli*. *Adv. Microb. Physiol.* 68, 433–507. doi: 10.1016/bs.ampbs.2016.02.008

Sato, M., Mori, Y., and Iida, T. (1992). Convenient synthesis of N,N,N',N'-tetrakis(2-pyridylmethyl)-α,ω-alkanediamines using a phase-transfer catalyst. *Synthesis* 539–540. doi: 10.1055/s-1992-26157

Schaefer, A., Horn, H., and Ahlrichs, R. (1992). Fully optimized contracted Gaussian basis sets for atoms lithium to krypton. *J. Chem. Phys.* 97, 2571–2577. doi: 10.1063/1.463096

Schenk, G., Mitić, N., Hanson, G. R., and Comba, P. (2013). Purple acid phosphatase: a journey into the function and mechanism of a colourful enzyme. *Coord. Chem. Rev.* 257, 473–482. doi: 10.1016/j.ccr.2012.03.020

Schenk, G., Peralta, R. A., Batista, S. C., Bortoluzzi, A. J., Szpoganicz, B., Neves, A., et al. (2008). Probing the role of the divalent metal ion in uteroferrin using metal ion replacement and a comparison to isostructural biomimetics. *J. Biol. Inorg. Chem.* 13, 139–155. doi: 10.1007/s00775-007-0305-z

Schultz, B. E., Ye, B.-H., Li, X.-Y., and Chan, S. I. (1997). Electronic paramagnetic resonance and magnetic properties of model complexes for binuclear active sites in hydrolase enzymes. *Inorg. Chem.* 36, 2617–2622. doi: 10.1021/ic960988r

Selleck, C., Clayton, D., Gahan, L. R., Mitić, N., McGeary, R. P., Schenk, G., et al. (2017). Visualization of the reaction trajectory and transition state in a hydrolytic reaction catalyzed by a metalloenzyme. *Chem. Eur. J.* 23, 4778–4781. doi: 10.1002/chem.201700866

Shaw, W. H. R. (1954). Inhibition of urease by various metal ions. *J. Am. Chem. Soc.* 76, 2160–2163. doi: 10.1021/ja01637a034

Shaw, W. H. R., and Raval, D. N. (1961). The inhibition of urease by metal ions at pH 8.9. *J. Am. Chem. Soc.* 83, 3184–3187. doi: 10.1021/ja01476a004

Sheldrick, G. M. (1997). *SHELXL97: Program for the Refinement of Crystal Structures.* Germany, University of Gottingen.

Shin, W., and Lindahl, P. A. (1992). Discovery of a labile nickel ion required for CO/acetyl-CoA exchange activity in the NiFe complex of carbon monoxide dehydrogenase from Clostridium thermoaceticum. *J. Am. Chem. Soc.* 114, 9718–9719. doi: 10.1021/ja00050a094

Sibille, J. C., Doi, K., and Aisen, P. (1987). Hydroxyl radical formation and iron-binding proteins. stimulation by the purple acid phosphatases. *J. Biol. Chem.* 262, 59–62.

Siluvai, G. S., and Murthy, N. N. (2009). X-ray structure and spectroscopic characterization of divalent dinuclear cobalt complexes containing carboxylate- and phosphodiester- auxiliary bridges. *Inorg. Chim. Acta* 362, 3119–3126. doi: 10.1016/j.ica.2009.02.010

Smith, S. J., Casellato, A., Hadler, K. S., Mitić, N., Riley, M. J., Gahan, L. R., et al. (2007). The reaction mechanism of the Ga(III)Zn(II) derivative of uteroferrin and corresponding biomimetics. *J. Biol. Inorg. Chem.* 12, 1207–1220. doi: 10.1007/s00775-007-0286-y

Smith, S. J., Riley, M. J., Noble, C. J., Hanson, G. R., Stranger, R., Gahan, L. R., et al. (2009). Structural and catalytic characterization of a heterovalent Mn(II)Mn(III) complex that mimics purple acid phosphatases. *Inorg. Chem.* 48, 10036–10048. doi: 10.1021/ic9005086

Spears, J. W., Smith, C. J., and Hatfield, E. E. (1977). Rumen bacterial urease requirement for nickel. *J. Dairy Sci.* 60, 1073–1076. doi: 10.3168/jds.S0022-0302(77)83990-8

Suzuki, M., Sugisawa, T., Senda, H., Oshio, H., and Uehara, A. (1989). Synthesis and characterization of a novel tetranuclear manganese(II,III,III,II) mixed valence complex. *Chem. Lett.* 1091–1094. doi: 10.1246/cl.1989.1091

Suzuki, M., Sugisawa, T., and Uehara, A. (1990). Dinuclear cobalt(II) complexes containing 1,3-(or 1,5-)bis[bis-(2-pyridylmethyl)amino]-2-propanolato (or−3-pentanolato): preparation and reaction with molecular oxygen. *Bull. Chem. Soc. Jpn.* 63, 1115–1120. doi: 10.1246/bcsj.63.1115

Tian, J.-L., Feng, L., Gu, W., Xu, G.-J., Yan, S.-P., Cheng, D.-P., et al. (2007). Synthesis, crystal structure, magnetic property and nuclease activity of a new binuclear cobalt(II) complex. *J. Inorg. Biochem.* 101, 196–202. doi: 10.1016/j.jinorgbio.2006.08.009

Tian, J.-L., Gu, W., Yan, S.-P., Liao, D.-Z., and Jiang, Z.-H. (2008). Synthesis, structures and magnetic properties of two binuclear cobalt(II) complexes bridged by bis(p-nitrophenyl) phosphate or diphenylphosphinate ion. *Z. Anorgan. Allgem. Chem.* 634, 1775–1779. doi: 10.1002/zaac.200800130

Tomkowicz, Z., Ostrovsky, S., Foro, S., Calvo-Perez, V., and Haase, W. (2012). Magnetooptical and structural investigations of five dimeric cobalt(II) complexes mimicking metalloenzyme active sites. *Inorg. Chem.* 51, 6046–6055. doi: 10.1021/ic202529p

Tudor, V., Marin, G., Lloret, F., Kravtsov, V. C., Simonov, Y. A., Andruh, M., et al. (2008). New alkoxo-bridged mixed-valence cobalt clusters: synthesis, crystal structures and magnetic properties. *Inorg. Chim. Acta* 361, 3446–3452. doi: 10.1016/j.ica.2008.03.007

Vaissier, V., and Van, V. T. (2017). Quantum chemical approaches to [NiFe] hydrogenase. *Essays Biochem* 61, 293–303. doi: 10.1042/EBC20160079

Vichard, C., and Kaden, T. A. (2002). Phosphate and phosphonate ester hydrolysis promoted by dinuclear metal complexes. *Inorg. Chim. Acta* 337, 173–180. doi: 10.1016/S0020-1693(02)00997-0

Vichard, C., and Kaden, T. A. (2004). Phosphate diester hydrolysis in biological relevant compounds by dinuclear metal complexes. *Inorg. Chim. Acta* 357, 2285–2293. doi: 10.1016/j.ica.2003.12.041

Wages, H. E., Taft, K. L., and Lippard, S. J. (1993). Tris(acetato)bis(N,N,N',N'-tetramethylethylenediamine)(urea)dinickel(1+) triflate and [Ni(OAc)(urea)2(tmen)](OTf), model complexes for the enzyme urease. *Inorg. Chem.* 32, 4985–4987. doi: 10.1021/ic00075a001

Wu, A.-Z., and Wang, T. (2014). Synthesis, crystal structures and phosphodiesterase activities of alkoxide-bridged asymmetric dinuclear nickel(II) complexes. *Trans. Met. Chem.* 39, 205–211. doi: 10.1007/s11243-013-9791-8

Xavier, F. R., and Neves, A. (2016). Synthesis, physicochemical properties and *in vitro* catalytic activity of a dinuclear nickel(II) complex with a N5O-hexadentate ligand: a functional model for phosphohydrolases. *Polyhedron* 109, 59–66. doi: 10.1016/j.poly.2016.02.013

Yamaguchi, K., Akagi, F., Fujinami, S., Suzuki, M., Shionoya, M., and Suzuki, S. (2001). Hydrolysis of phosphodiester with hydroxo- or carboxylate-bridged dinuclear Ni(II) and Cu(II) complexes. *J. Chem. Soc. Chem. Commun.* 375–376. doi: 10.1039/b008994j

Yamaguchi, K., Koshino, S., Akagi, F., Suzuki, M., Uehara, A., and Suzuki, S. (1997). Structures and catalytic activities of carboxylate-bridged dinickel(II) complexes as models for the metal center of urease. *J. Am. Chem. Soc.* 119, 5752–5753. doi: 10.1021/ja963982+

Yamane, H., Hosokawa, Y., Nakao, Y., Matsumoto, K., Takamizawa, S., Mori, W., et al. (1997). Dinuclear nickel(II) complexes as models for the active site of urease. *J. Inorg. Biochem.* 67:186. doi: 10.1016/S0162-0134(97)80063-3

Yamane, H., Nakao, Y., Kawabe, S., Xie, Y., Kanehisa, N., Kai, Y., et al. (2001). Synthesis, structures and characterization of the dinuclear nickel(II) complexes containing N,N,N',N'-tetrakis[(1-ethyl-2-benzimidazolyl)methyl]-2-hydroxy-1,3-diaminopropane and their urea complexes relevant to the urease active site. *Bull. Chem. Soc. Jpn.* 74, 2107–2112. doi: 10.1246/bcsj.74.2107

Zambelli, B., Musiani, F., Benini, S., and Ciurli, S. (2011). Chemistry of Ni^{2+} in Urease: Sensing, Trafficking, and Catalysis. *Acc. Chem. Res.* 44, 520–530. doi: 10.1021/ar200041k

Zeng, M.-H., Gao, S., and Chen, X.-M. (2004). A novel 3D coordination polymer containing pentacoordinate cobalt(II) dimers with antiferromagnetic ordering. *Inorg. Chem. Commun.* 7, 864–867. doi: 10.1016/j.inoche.2004.05.008